RESULTS OF ICARUS 9 EXPERIMENTS RUN AT IMRA EUROPE

T. Roulette, J, Roulette, and S. Pons

IMRA Europe, S.A., Centre Scientifique
Sophia Antipolis, 06560 Valbonne , FRANCE

INTRODUCTION

We describe herein the construction, testing, calibration and use of a high power dissipation calorimeter suitable for the measurements of excess enthalpy generation in Pd / Pd alloy cathodes during the electrolysis of heavy water electrolytes at temperatures up to and including the boiling point of the electrolyte. With the present design, power dissipation up to about 400W is possible. Excess power levels of up to ~250% of the input power have been observed with these calorimeters in some experiments. Extensions of the design to include recombination catalysts on open and pressurized cells will be the subject of a future report.

DESIGN AND EXPERIMENTAL CONSIDERATIONS

A schematic diagram of the basic construction of the calorimeter is shown in Figure 1. These

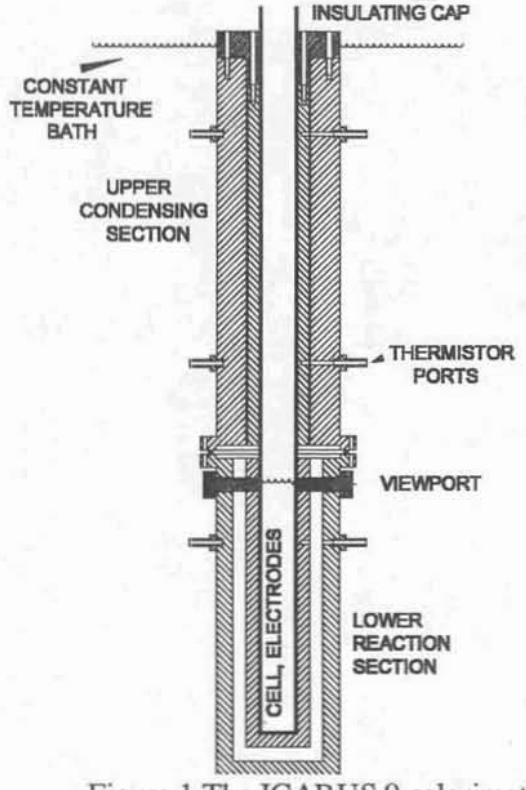

Figure 1 The ICARUS 9 calorimeter

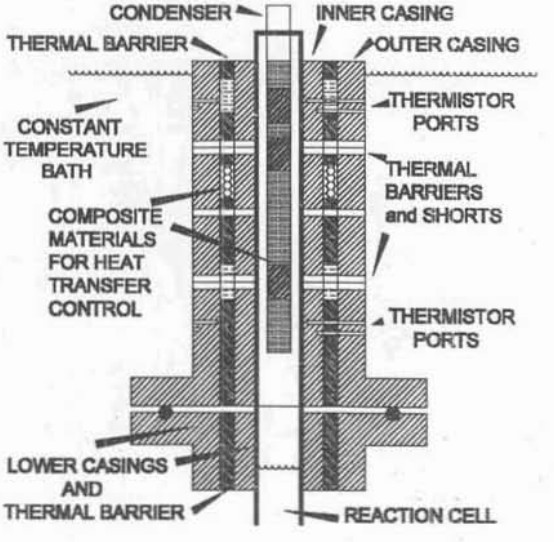

Figure 2 Top section expanded details

calorimeters are much improved in thermal dissipation, sensitivity, precision, and accuracy compared to the original calorimeters used in these laboratories from 1992 to 1995. The present design

incorporates better seals at all liquid / casing interfaces, and at the thermistor inlet ports. The viewing ports are also more robust and clear. The heat transfer characteristics can now be easily be modified at various vertical positions in the inner casing, the inner insulator, and the internal condenser to give more controllable overlap between the various sensitivity zones, Figure 2. The resulting heat transfer characteristics are now more linear in the radial direction than in previous designs. Foam rise in the calorimeter at the boiling temperature has been minimized.

In the basic configuration, there are three sets of differential temperature measuring thermistors at key vertical locations in the inner and outer casings so that the radial temperature distribution throughout the calorimeter can be characterized conveniently and accurately. The cell potential, cell current, and cell temperature are measured independently, Figures 3-5.

The principle of operation of these calorimeters is straightforward. Power dissipation in the cell is determined by measuring the differences in temperature between the thermistor sets as a function of input power. Excess enthalpy generation is calculated by comparing the data to those obtained by calibration as described below. It is pointed out that these calorimeters have been used thus far primarily for measurements in the steady state, i.e. when the input power levels, bath temperature, and the rates of electrochemical and ohmic enthalpy generation in the cell are constant. Under these conditions, thermal equilibrium is attained in all sections of the calorimeter. Extensions to measurements in the non-steady state are necessary for larger devices, and are certainly possible (these are beyond the scope of the present report).

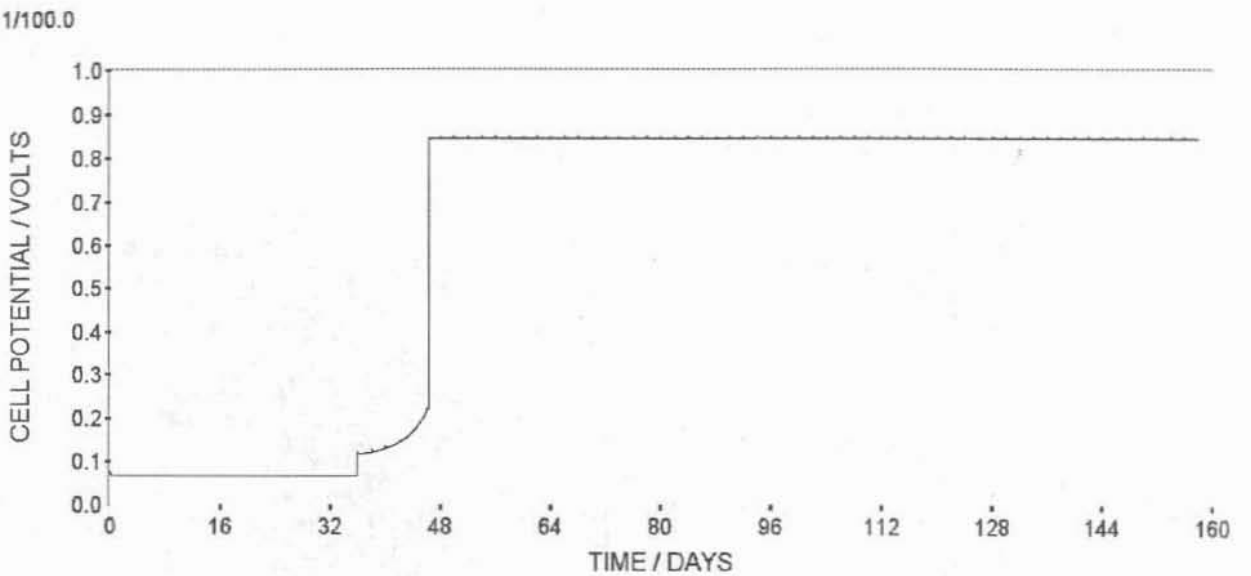

Figure 3 Measured cell voltage as a function of time for the duration of the experiment. All data presented in this report are for experiment #4 described in the Table at the end of this report.

The casings in the top section (measuring / condensing section) are thermally isolated from the lower section (reaction section). As the temperature due to an electrochemical reaction in the cell in the bottom section rises, heat is transferred to the upper section primarily by (a) heat contained in the vapor of the solvent rising from the lower section, and (b) by conduction through the walls of the glass reaction cell. We consider that the overall effects of (b) is small compared to effect (a), especially when the contents of the reaction cell are at or near the boiling point. The calorimeter was initially designed primarily for measurements when the cell contents are boiling, but the calorimeter is indeed suited for measurements at all temperatures below the boiling point. In the basic configuration (simple solid casings and insulation) the lower set of thermistors are the most accurate at lower temperatures since they are located closer to the top surface of the solvent. The middle and upper sets of thermistors are located in the upper section, and these are more sensitive as the temperature

rises towards boiling.

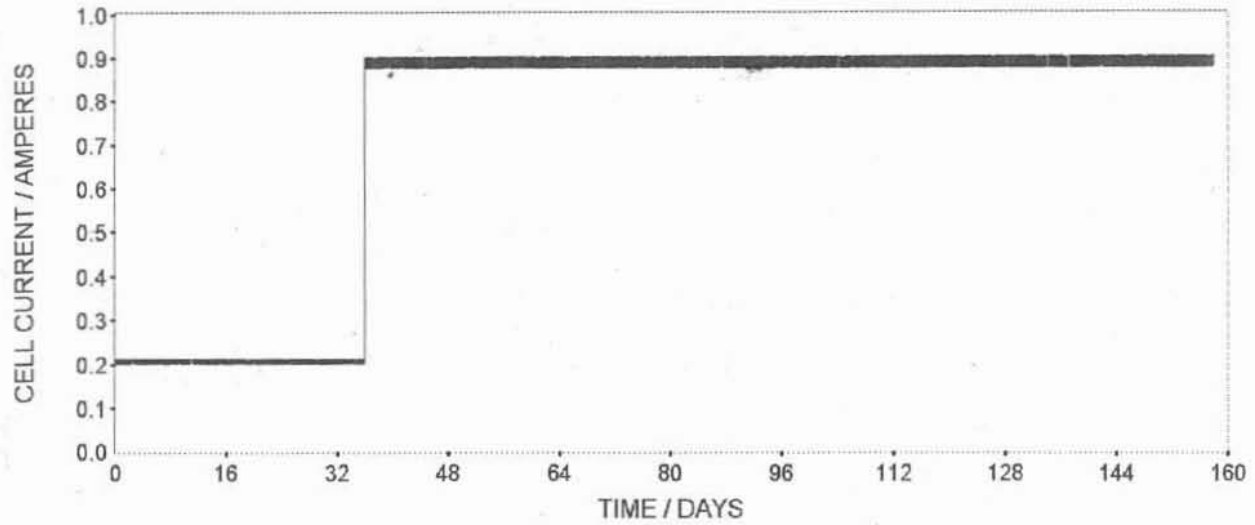

Figure 4 Cell current as a function of time.

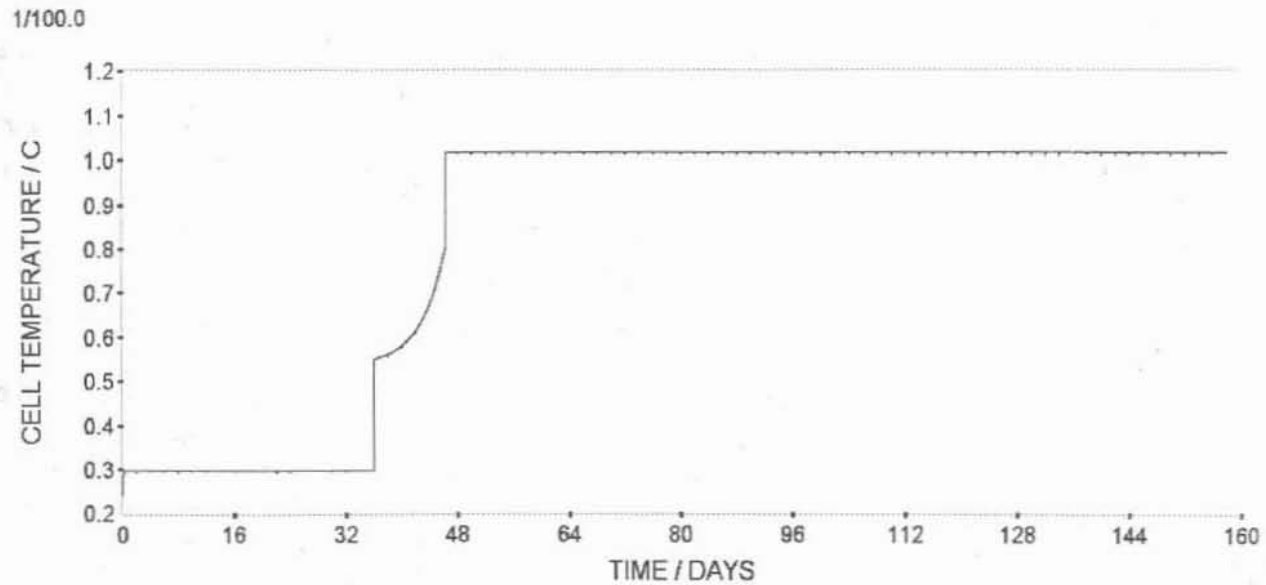

Figure 5 Internal cell temperature as a function of time.

As the temperature of the solvent rises, the vapor pressure of the fluid also rises and the temperature of the vapor increases progressively in the upper portions of the calorimeter. At boiling, the temperature of the vapor just above the liquid is at the boiling point of the solvent. If the rate of boiling is increased, due either to increased external power input or to excess heat generation, the rate of boiling increases and the height of the hot vapor head rises to increasingly higher levels in the calorimeter. Since the temperature of the vapor cannot exceed the temperature of the boiling liquid at a given atmospheric pressure, the temperature measured at any inner casing thermistor can not exceed the boiling point of the solvent. Therefore, if the bath temperature remains constant, then the temperature difference measured between the inner and outer thermistor of each set will rise to a maximum value, which is independent of the power input level. When this maximum is reached, any increases in the power in the bottom of the cell will have no further effect on the measured temperature difference. For this reason, in the basic configuration, the lower thermistor set is

sensitive only at low temperatures (up to about 30 watts of power dissipation in the reaction cell). At higher powers, there is no further changes in the temperature difference at this lower set of thermistors. The middle set of thermistors then become more sensitive, and at very high power dissipation rates, the upper set of thermistors become more sensitive. In other configurations, it is possible to modify the sensitivity of each thermistor set by changing the materials and construction of the internal condenser plug and/or the inner casing, as well as placing annular ring insulators at various heights of the inner casing, and/or thermal shorting devices between the inner and outer section casings. Finally, similar enhancements are obtained by changing the materials in, and the geometry of the insulating barrier between the inner and outer casings, Figure 2.

Due to these operating characteristics, it will be noticed in some of the figures that there are high or low calculated rates of excess enthalpy generation at very low power inputs, especially at the middle and upper thermistor sets. These data must be ignored since they are due to the systematic errors described further below.

The calorimeters are calibrated by several methods, including (a) the electrolysis of (i) light water or (ii) heavy water using Pt cathodes, and (b) encapsulated and open platinum resistor heaters. At thermal equilibrium, the input power and the temperature differences at each set of thermistors is measured over a long time period. The procedure for calibration calls for the application of fixed input powers to the cell for approximately 12 hours. The time constant of the calorimeter is considerably less than this time period, so one obtains a large number of steady state calibration points from which a good statistical average value can be obtained. Gaussian statistics are used to determine histograms and probability functions on each set of input power and temperature difference data sets for each point and for each thermistor set. Non-steady state values at short times after the input power is changed are rejected on the basis of their contribution to the known determinate error (the non-steady state). Rejection of data is continued (up to about 10% of the entire data set) until a zero slope linear fit is found for the temperature difference as a function of input power. The intercept of this line then gives the "best" temperature difference value. Confidence limits and prediction limits are then determined for each set of data. Inflection points for the confidence and prediction curves are then determined, which gives a "best" value of the input power. Gaussian histograms and cumulative curves are additionally determined, from which the "best" mean value of both the temperature difference values and the input power values. If these are in agreement with the values determined by the previous method, then they are accepted. If not, they are rejected and the measurements are repeated. Generally, calibrations are always very reliable at power inputs above about 3W. When the calorimeter is serviced after each experiment, the calibration curves are carefully checked by re-calibration at several input powers to assure that the calibrations have not changed during the prior operating or servicing period.

Following this procedure, calibrations curves are constructed over the entire input power range of the calorimeter for each of the thermistor sets. For simplicity in on-line data monitoring, best fit curves are calculated by linear and non-linear regression analysis over various sections of the calibration data. We use a variety of basis trial models such as Boltzman, multiple exponential, sigmoidal Gompertz, sigmoidal logistical, Weibull, Richards, and Hill functions. The calibration curves shown in this report were obtained from such composite best fit curves through all of the experimental calibration power / temperature data, and then plotted at integer values of the input power. Segments to these curves are almost always added to these curves for very low values (<2-3W) of input power since the error between the actual values and fitted curves were about 5%.

During an experiment, measurements identical to those used in the calibration method are made, and the temperature differences between the three sets of thermistors are compared with those of the blanks, at the same input power level, see, for example, Figure 6 . If there are any excess enthalpy effects, then the data points will fall above the input power - thermistor difference temperature calibration lines. The horizontal distance from a high data point to the calibration line to the right gives the value of the excess enthalpy generation rate. Excess enthalpy effects cannot be

observed at high temperatures at the bottom thermistor set. Figures 7-9 reflect these calculated rates of excess power generation at each of the three thermistor sets. Derived analyses may then be calculated from these data: for example the excess power percentage of input power, the excess energy, and the accumulated excess energy as a function of time; see Figures 10 and 11.

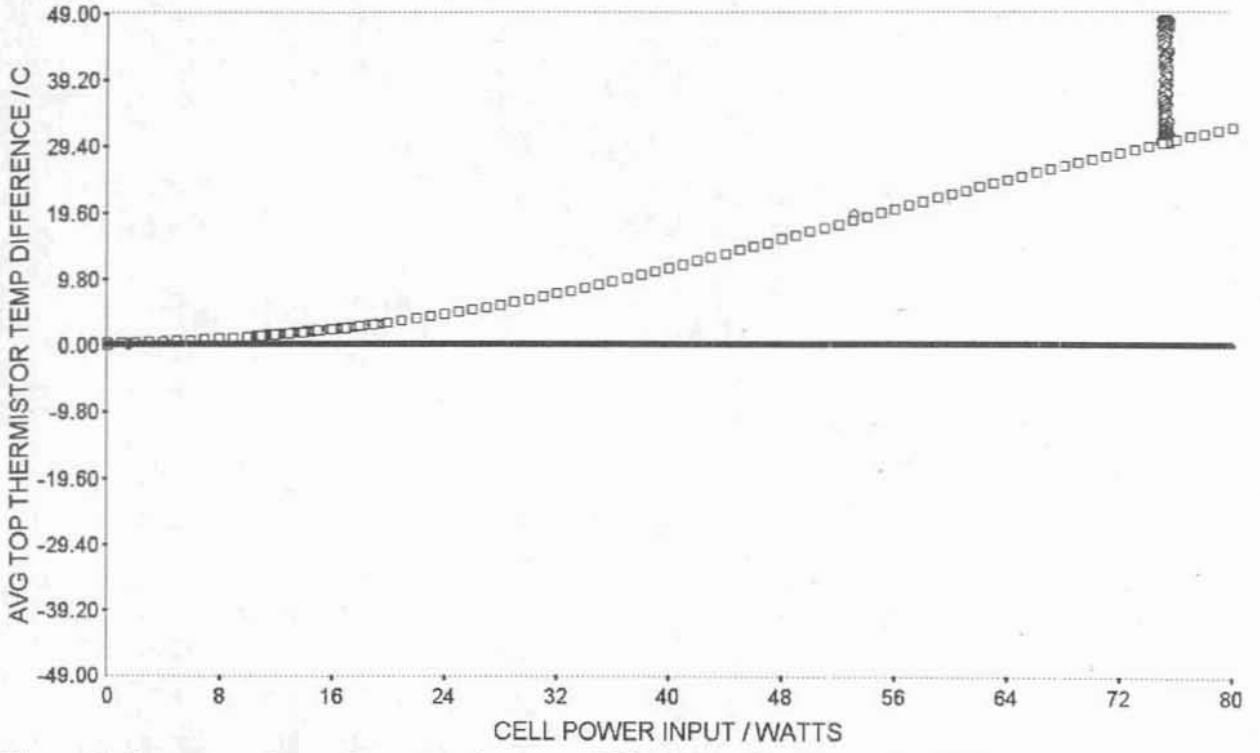

Figure 6 Average values of consecutive sets of 25 points of temperature differences at the top set of thermistors as a function of the average cell input power. Calibration: squares; Data: circles.

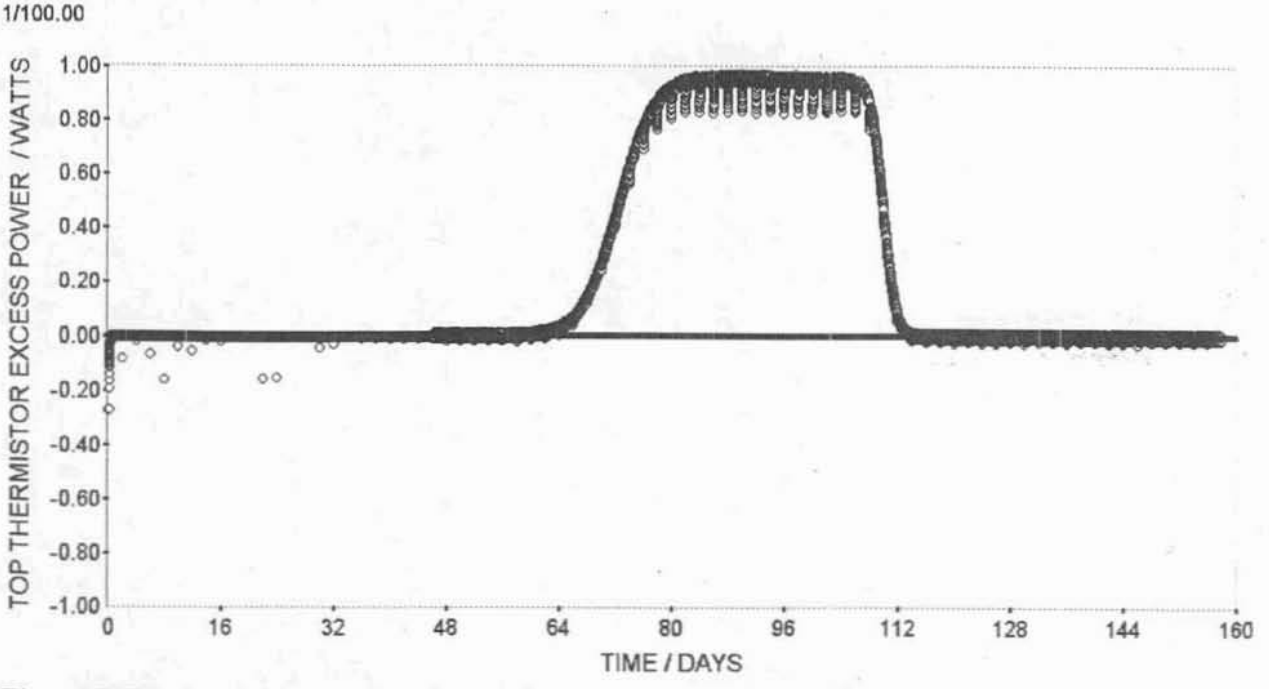

Figure 7 Excess power as a function of time measured at the top thermistor set.

Excess Heat

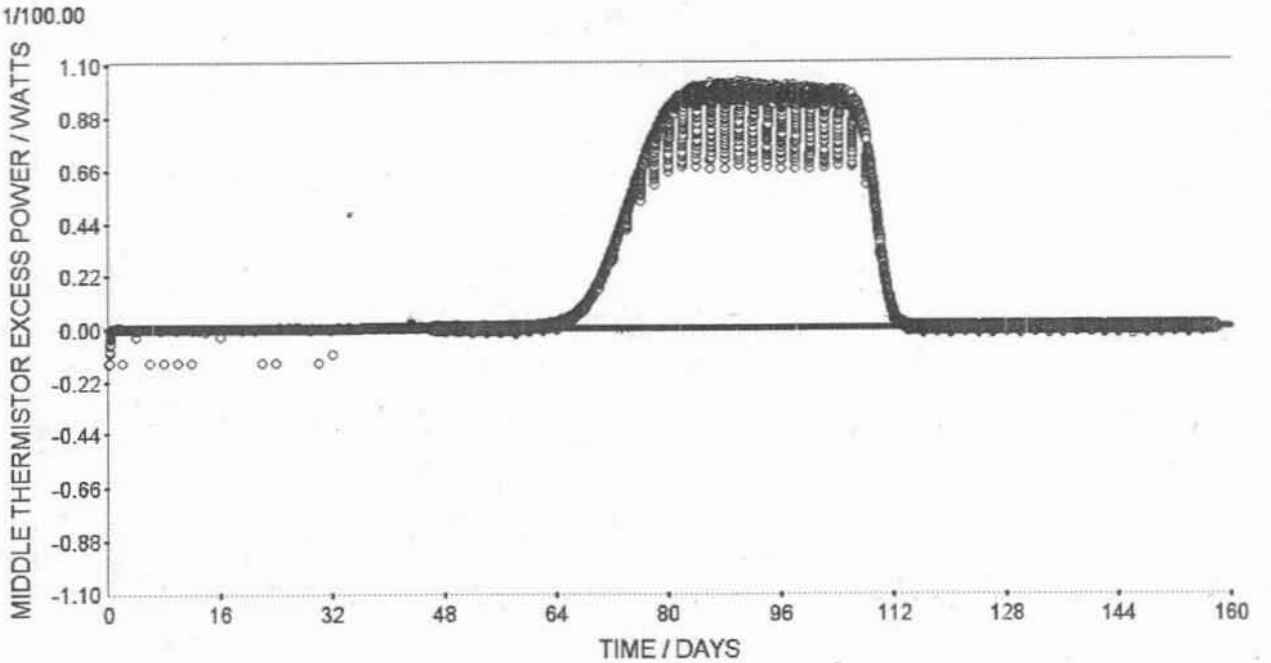

Figure 8 Excess power as a function of time measured at the middle thermistor set.

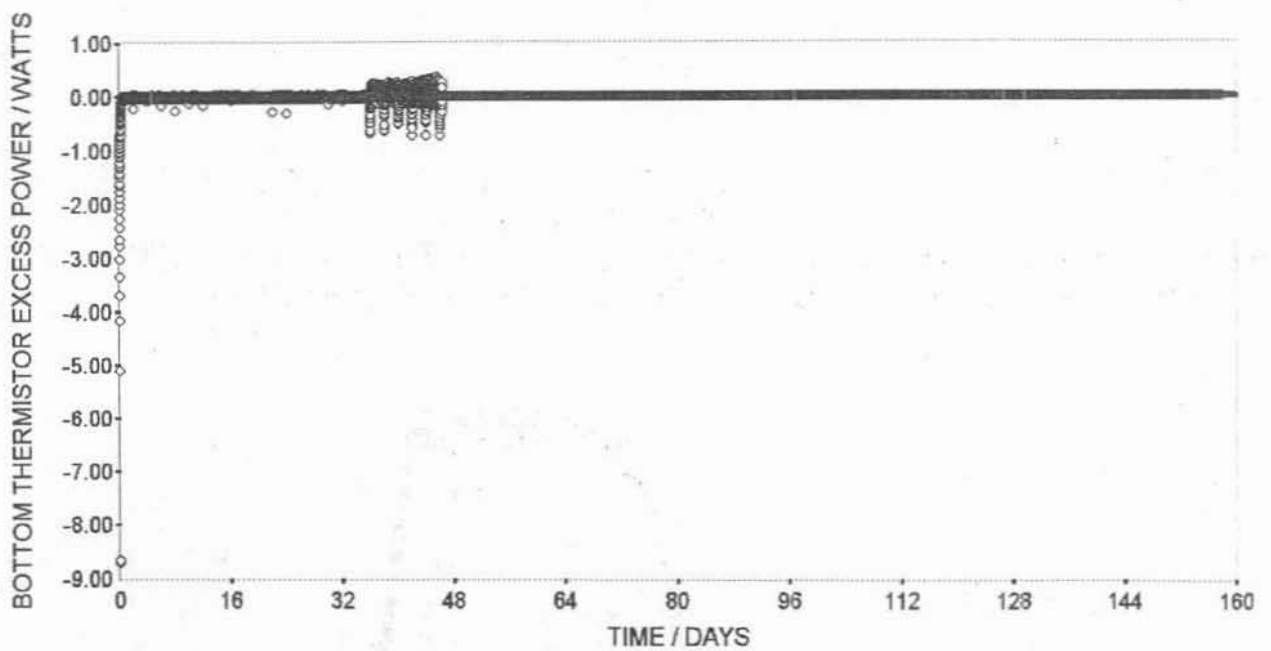

Figure 9 Excess power as a function of time measured at the bottom thermistor set.

It has been pointed out previously that there can be anomalous values of excess heat or cooling observed in these experiments. Such anomalies are seen in the experimental response curves for each of the top, middle, and bottom thermistor pairs. These anomalies must always occur during periods of the non-steady state which may be imposed externally or internally on the experiment. Low anomalous values of heat generation (i.e. cooling) must appear during (a) the period immediately following the addition to the cell of solvent which is colder than the cell contents, (b) the period immediately following an increase in the input power, (c) the period immediately following an increase in the bath temperature, and in general, (d) the period immediately following any event in which the interior casing of the calorimeter becomes cooler with respect to the exterior casing and which does not result in an exactly compensating decrease in the input power

Anomalous high values of excess heat must be observed during (a) the period immediately

following the addition to the cell of solvent which is warmer than the cell contents, (b) the period immediately following an decrease of the power input to the cell, (c) the period immediately

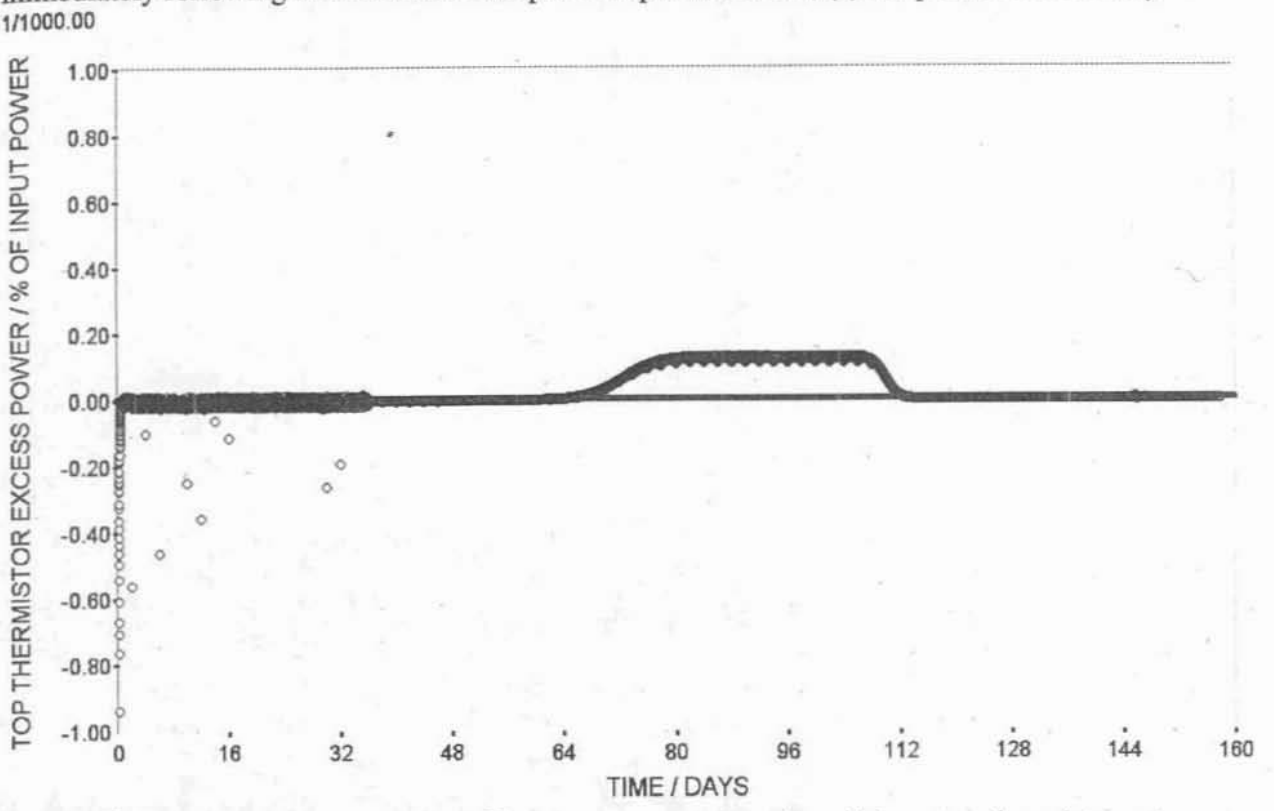

Figure 10 Excess power percentage of input power as a function of time: top thermistor set.

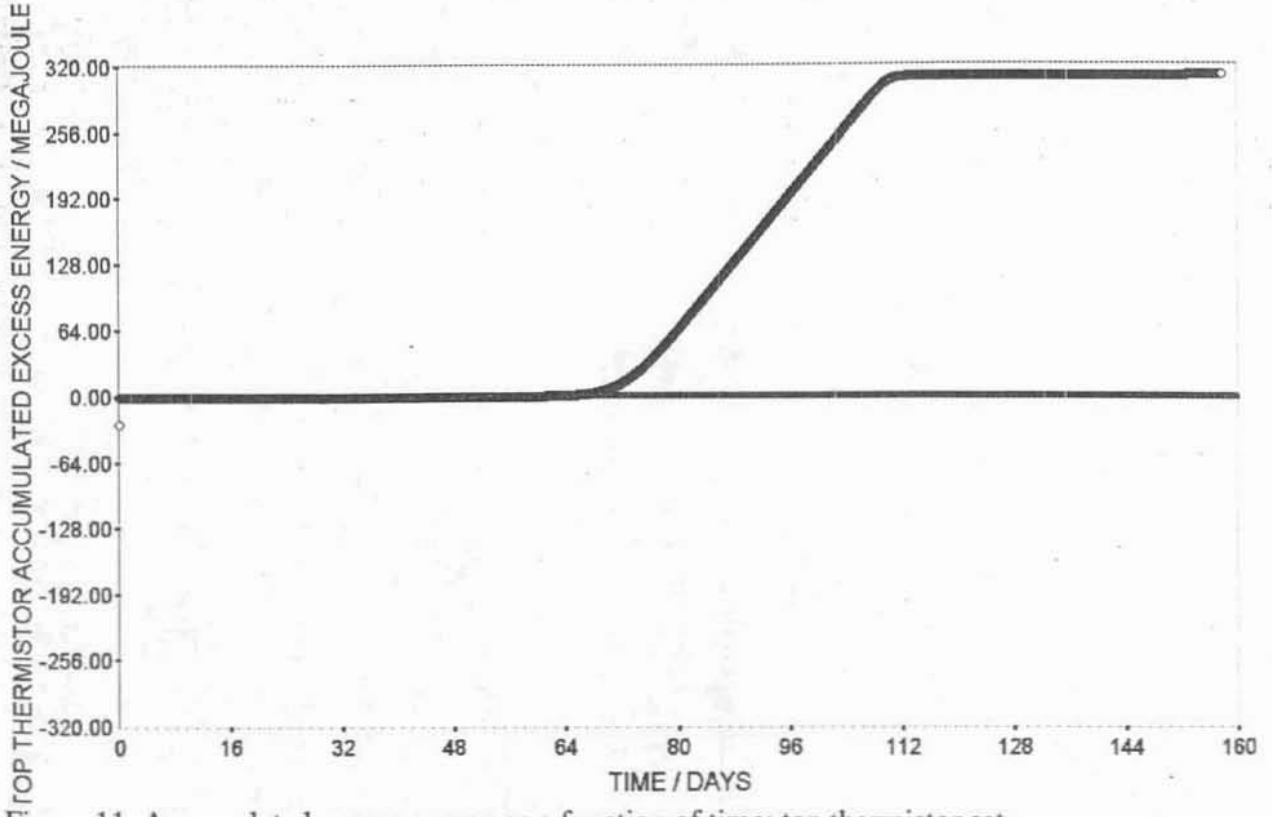

Figure 11 Accumulated excess energy as a function of time: top thermistor set.

following a decrease in the bath temperature, (d) the period immediately following the onset of any excess enthalpy generation in the cell, and in general, (e) the period immediately following any event

Excess Heat

in which the interior casing of the calorimeter becomes warmer with respect to the exterior casing and which does not result in an exactly compensating increase in the input power.

Each of the perturbations listed in the last paragraph are non-equilibrium effects. Attention therefore is normally focused only to those data which are recorded when the cell is known to be at thermal equilibrium, i.e. at the majority of the data points in the experiments reported here.

One is also cognizant of the fact that non-equilibrium effects may also be imposed by ambient conditions of the laboratory environment on the components of the cell which pass from the calorimeter into the ambient air, such as cables and leads, the glass lead tubes, the plastic plugs, and the plastic condenser. Conduction effects can certainly affect the stability of the measurements. For this reason, the fluctuation of the air temperature in the laboratory is always maintained to +/- 0.15°C, and within +/- 0.5°C of the bath temperature. The fluctuations are therefore reduced to negligible values, and there are observable fluctuations of +/- 0.05°C only at very low power inputs and at the top thermistor only.

The table below summarizes the last set of 7 experiments undertaken with the new calorimeter system at IMRA Europe. As can be seen, the experiments fall into two clear categories of success or failure. Long charging times at low current densities, and careful experimental protocols are always utilized in the experiments, and tend to increase the success rate of excess enthalpy generation. However, the necessary condition for excess enthalpy generation remains the quality and preparation of the cathode materials and electrolyte. A more careful investigation of the materials properties and preparation continues, and these studies have certainly led to increased excess enthalpy generation rates for longer periods of time. These studies will be detailed in our future reports.

Experiment	1	2	3	4	5	6	7
Cathode	Pd	Pd	Pd	Pd	Pd	Pd	Pd
Rod size, mm	100x2	100x2	100x2	100x2	100x2	12.5x2	12.5x2
Anode	Pt coil	Pt coil	Pt coil	Pt coil	Pt coil	Pt mesh	Pt mesh
Electrolyte:0.1M	LiOD	LiOD	LiOD	LiOD	LiOD	LiOD	LiOD
Electrolyte, mL:	90.7	90.0	90.6	97.0	97.0	90.4	90.9
Expt time, days	94	134	158	123	123	47	60
Pwr_{excess}/W/4.2hr	-0.1	-0.6	101	17.3	13.8	74.5	39.4
Total energy, MJ	-0.0	-5.5	294	102	0.3	30.5	-7.6
% excess power	0	0	150 (30d)	250 (70d)	0	Variable	~0